

Protein engineering of oxidosqualene-lanosterol cyclase into triterpene monocyclaset†

Cite this: *Org. Biomol. Chem.*, 2013, **11**, 4214

Cheng-Hsiang Chang, Hao-Yu Wen, Wen-Shiang Shie, Ching-Ting Lu, Meng-Erh Li, Yuan-Ting Liu, Wen-Hsuan Li and Tung-Kung Wu*

A computational modeling/protein engineering approach was applied to probe H234, C457, T509, Y510, and W587 within *Saccharomyces cerevisiae* oxidosqualene-lanosterol cyclase (ERG7), which spatially affects the C-10 cation of lanosterol formation. Substitution of Trp587 to aromatic residues supported the "aromatic hypothesis" that the π -electron-rich pocket is important for the stabilization of electron-deficient cationic intermediates. The Cys457 to Gly and Thr509 to Gly mutations disrupted the pre-existing H-bond to the protonating Asp456 and the intrinsic His234: Tyr510 H-bond network, respectively, and generated achilleol A as the major product. An H234W/Y510W double mutation altered the ERG7 function to achilleol A synthase activity and generated achilleol A as the sole product. These results support the concept that a few-ring triterpene synthase can be derived from polycyclic cyclases by reverse evolution, and exemplify the power of computational modeling coupled with protein engineering both to study the enzyme's structure–function–mechanism relationships and to evolve new enzymatic activity.

Received 11th March 2013,
Accepted 24th April 2013

DOI: 10.1039/c3ob40493e

www.rsc.org/obc

Introduction

Computational modeling/protein engineering techniques have paved the way to understand enzyme's structure–function–mechanism relationships and to render novel functions. We previously applied the strategy to investigate the effects of amino acid substitutions on the cyclization mechanism and product profile of the *Saccharomyces cerevisiae* oxidosqualene-lanosterol cyclase (ERG7), a fascinating enzyme which catalyzes the cyclization/rearrangement of acyclic (3*S*)-2,3-oxidosqualene (**OS**, **1**) to tetracyclic lanosterol (**LA**, **2**).^{1–4} The reaction for **LA** formation proceeds through a prefolded chair–boat–chair (C–B–C) substrate conformation, followed by an oxirane ring protonation and cleavage, four consecutive carbocation-mediated ring annulations and 1,2-shifted hydride/methyl group migrations, and a specific deprotonation. Several plasticity residues within either the first- or second-tier active site of ERG7 have been identified to influence the cyclization/rearrangement cascade and generate diverse truncated and rearranged products.^{5–19}

Genome sequencing and functional analyses of oxidosqualene cyclases from various species suggested that although polycyclic oxidosqualene cyclases can be evolved from

enzymes that form smaller ring systems by iterative addition of motifs that favor additional rings, there may exist a reverse evolutionary order of polycyclic cyclases into fewer-ring triterpene cyclases.²⁰ For example, phylogenetic analysis indicates that camelliol C synthase (CASM1) is a descendent of LUP clade enzymes that form pentacyclic amyirin or lupeol.²⁰ In addition, ring annulations of **OS** to a rearranged bicyclic intermediate with a rare evolutionary transition from a B-ring chair to B-ring boat conformation, catalyzed by a marnerial synthase (MRN1) from *Arabidopsis thaliana*, indicates that MRN1 arose within the eudicot PEN clade from enzymes that generate the all-chair dammarenyl cation.²¹ Furthermore, molecular cloning of an oxidosqualene cyclase to produce a C-ring seco-triterpenes supported direct production of other natural seco-triterpenes by the same enzyme.²² Recently, functional characterization of an achilleol B synthase from *Oryza savita* suggested that achilleol B synthase shares the same clade as β -amyirin synthase from *Avn strigosa*.²³ These results demonstrated the potential for reverse evolution of polycyclic triterpene cyclases into monocyclic or few-ring triterpene cyclases through computational modeling coupled with protein engineering.

Achilleol A (**3**), a monocyclic triterpenoid, was first isolated from *Achillea odoranta* and later found to co-occur with the sesquiterpenoid elegansidiol.²⁴ The biosynthesis of **3** could be achieved either by **OS** monocyclization or by tail-to-tail condensation of monocyclic and acyclic sesquiterpenes.²⁴ In parallel, the biosynthesis of **3** is of considerable interest both in

Department of Biological Science and Technology, National Chiao Tung University, 300, Hsin-ChuTaiwan, Republic of China. E-mail: tkwmll@mail.nctu.edu.tw
†Electronic supplementary information (ESI) available. See DOI: 10.1039/c3ob40493e

considerations of biological activities, and of the OSC-catalyzed cyclization mechanism (concerted or non-concerted).^{25,26} Previous studies on ERG7 showed that the Tyr510 residue is involved both in influencing monocyclic to tetracyclic product formation and in stabilizing the C-8/C-9 cation for deprotonation, and that the His234 residue is involved in influencing deprotonation *via* a H-bonding network to the hydroxyl group of the Tyr510. Specifically, site-directed mutation of Tyr510 to Lys or Trp produced achilleol A and camelliol C in ratios of 86:14 and 96:4, respectively.¹⁰ Furthermore, the His234 to Trp mutation produced minor amount of parkeol as the sole product.¹³ These observations suggested that steric or electrostatic interaction between these two residues might play a functional role in determining the deprotonation step for monocyclic or few-ring product formation, or altered deprotonation.

Results and discussion

To further explore the plasticity residues putatively involved in OS A-ring cyclization and to engineer oxidosqualene cyclase into achilleol A synthase, we mutated five amino acid residues that spatially putatively affect the C-10 cation of **2**, based on homology model of ERG7, and characterized the product profiles. Careful examination of the homology model suggested that all residues are positioned on top half of the active site cavity except for Trp587, which is located on the floor of the active site. The ERG7^{C457X}, ERG7^{T509X}, ERG7^{Y510X}, and ERG7^{W587X} site-saturated and ERG7^{Y510X/W234X} double site-directed mutations were constructed, using the QuikChange site-directed mutagenesis kit, and transformed into a yeast TKW14 strain for genetic selection and product characterization, as previously described.^{10,13} The genetic selection results showed that all W587X mutations resulted in non-viable TKW14[pERG7^{W587X}] mutants, except for the Phe and Tyr substitutions (Table S1†). These results indicated that the Trp587 mutations were detrimental to the essential activity of ERG7, except for the Phe and Tyr substitutions. Alternatively, small, uncharged, or non-polar aliphatic amino acid substitutions at Cys457 and Thr509 positions maintained the cyclase activity, whereas the aromatic, acidic, or basic amino acid substitutions are unable to complement the ERG7 disruption. These results indicated that the Cys457 and Thr509 mutations are not essential to the catalytic activity of ERG7, but play some functional role during the catalytic process. The Tyr510 to Lys, Arg, Thr, Pro, and Trp mutations failed to complement the ERG7 activity in the absence of exogenous ergosterol. The Tyr510 and His234 to Trp double mutations were also non-viable without exogenous ergosterol supplementation.

Following genetic selection with ergosterol complementation experiments, the non-saponifiable lipids (NSLs) from each mutant were extracted and purified using a AgNO₃-impregnated silica gel column for product profile characterization, using GC-MS and NMR (¹H, ¹³C NMR, DEPT, ¹H-¹H COSY, HMQC, HMBC, and NOE) spectroscopic techniques. The

Table 1 The product profiles of ERG7 mutants and ERG7^{H234X/Y510X} double mutants

Mutant	2	3	4	5	6	7	8
ERG7	100	—	—	—	—	—	—
ERG7 ^{W587Y}	89.7	—	—	6.2	—	4.1	—
ERG7 ^{W587F}	78.8	—	0.8	7.6	2.3	10.5	—
ERG7 ^{C457G}	25.4	74.6	—	—	—	—	—
ERG7 ^{T509G}	85.2	10.6	—	—	—	—	4.2
ERG7 ^{Y510A}	39.0	27.0	—	—	—	34.0	—
ERG7 ^{Y510L}	74.0	—	26.0	—	—	—	—
ERG7 ^{Y510S}	40.0	—	4.0	—	—	56.0	—
ERG7 ^{Y510C}	33.0	—	67.0	—	—	—	—
ERG7 ^{Y510H}	5.0	45.0	24.0	—	—	26.0	—
ERG7 ^{Y510K}	—	87.0	—	—	—	—	13.0
ERG7 ^{Y510W}	—	94.0	—	—	—	—	6.0
ERG7 ^{H234W/Y510V}	90.0	2.0	8.0	—	—	—	—
ERG7 ^{H234W/Y510W}	—	100.0	—	—	—	—	—

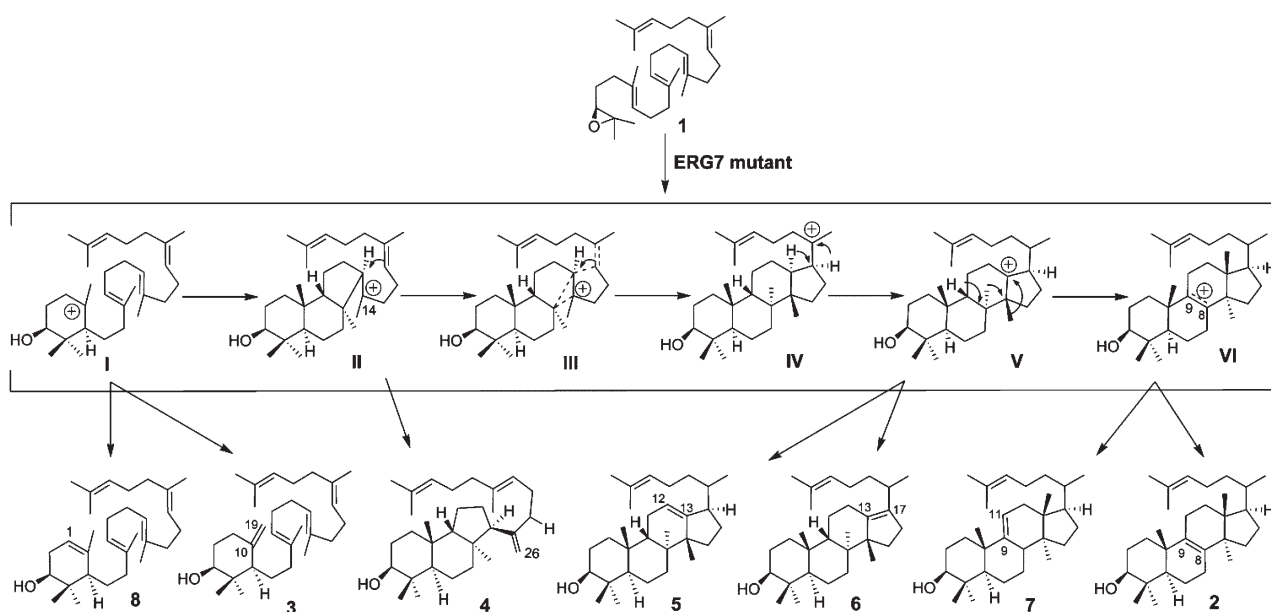
product profiles of the ERG7^{C457X}, ERG7^{T509X}, ERG7^{Y510X}, and ERG7^{W587X} site-saturated and ERG7^{Y510X/W234X} double site-directed mutations with molecular mass of 426 Da were listed in Tables 1 and S1.† Consistent with the genetic selection results, no products with *m/z* = 426 were observed for the W587X non-viable mutants. The GC-MS analyses and product comparison to authentic samples showed a large amount of lanosterol (**2**) and minor amounts of 13 α H-isomalabarica-14(26),17E,21-trien-3 β -ol (**4**), protosta-12(13),24-dien-3 β -ol (**5**), protosta-13(17),24-dien-3 β -ol (**6**), and parkeol (**7**) in the product profiles of the ERG7^{W587Y} and ERG7^{W587F} mutants.^{12,15–19} Interestingly, products derived from the W587F and W587Y mutations affected both chair-boat (C-B) 6-6-5 tricyclic Markovnikov C-14 and rearranged C-13/C-17 cationic stabilization, similar to the results of previously described Tyr99 and Phe699 site-saturated mutations.^{15,17,18} The Cys457 viable mutants produced **2** as the major product (>90%), except for Gly substitution, which produced **2** and **3** in a ratio of 25.4:74.6. The C457A, C457L, and C457T mutations also produced minor amounts of **4** and **7** or **4** alone. The production of **3** from the C457G mutation is reminiscent of MRN1, an oxidosqualene cyclase which also contains Gly in place of Cys and annulates OS to a bicyclic intermediate.²¹ For T509X mutations, no product was produced from the bulky or electrostatic substitutions such as T509Q, T509F, T509Y, and T509K mutations. The T509A, T509V, T509L, and T509N mutations produced **2** as the major product with various amounts of **4** and **7**. Interestingly, the T509G mutation produced **2**, **3**, and camelliol C (**8**) in a ratio of 85.2:10.6:4.2. The production of **3** and **8** from the T509G mutation suggested a spatial shift of Tyr510 position and/or an interference of the His234:Y510 H-bonding dyad to disrupt the process of bicyclic-ring formation to some extent. The non-viable ERG7^{Y510P/R/T} mutants produced neither **2** nor truncated intermediates, consistent with the genetic selection results. Nevertheless, the non-viable Y510K and Y510W mutations produced monocyclic **3** and **8** in the ratios of 87:13 and 94:6, respectively, without any polycyclic product formation. The viable Y510X mutants exhibited certain deprotonation profiles,

mainly monocyclic **3**, tricyclic **4**, altered deprotonated **7**, in conjunction with **2**. Neither truncated rearranged products derived from hydride or methyl group shift nor the altered deprotonation product from a C-7 cation could be identified. Most of the Y510X viable mutants, except the Y510A/L/S/C mutations, produced similar product profiles with different ratios. The Y510A mutation produced **2**, **3**, and **7** in ratios of 39.0 : 27.0 : 34.0, whereas the Y510L mutation generated **2** and **4** in a ratio of 74.0 : 26.0. No **3** was produced by Y510S or Y510C mutations. The Y510C mutation produced tricyclic compound **4** as the major product, whereas the Y510H mutation mainly terminated reaction at either the monocyclic or tricyclic position to yield **3** and **4** as major products. In addition, more monocyclic products were produced when Tyr510 was substituted with bulky or basic amino acids, whereas polycyclic products were observed with smaller or acidic amino acid substitution. We have previously shown that substitution of His234 with small non-polar hydrophobic residues facilitated the production of polycyclic products such as **5**, **7**, and protosta-20,24-dien-3 β -ol, but interfered with monocyclic **3** formation; whereas substitution of His234 with Tyr or Phe introduced steric hindrance or electrostatic repulsion to Tyr510, causing the shift of Tyr510 slightly out of active site pocket, and resulted in the production of **3** as well as other altered products. The H234W/Y510V double mutation yielded **2** : **3** : **4** in a ratio of 90 : 2 : 8. However, the H234W/Y510W double mutation produced **3** as the sole product.

A general mechanism for the ERG7-catalyzed OS cyclization/rearrangement pathway is shown in Scheme 1. A C-B-C prefolded OS within the enzyme active site underwent epoxide ring opening and subsequent A-ring annulation to generate the C-10 cation (**I**, lanosterol numbering). Subsequent abstraction of the proton from the C-25 and C-1 positions generated **3**

and **8** as the truncated products, respectively. In most cases, OS was cyclized to the tricyclic Markovnikov C-14 cation (**II**) as the first stopping point. Direct abstraction of proton from the C-26 methyl group of **II** yielded **4** as the truncated product. Alternatively, an anchimeric rearrangement and C-ring expansion from carbocation **III**, which was followed by D-ring annulation, generated protosteryl C-20 cation (**IV**). A series of two hydride rearrangement generated the lanosteryl C-13 cation (**V**). Elimination of a proton at C-12 or C-17 yielded product **5** or **6** as the end product, respectively. Then, two methyl-group shifts and a third hydride shift generated the lanosteryl C-8/C-9 cation (**VI**), which undergoes deprotonation at C-9 or C-8 to form **2** (Scheme 1).²⁷

The homology structural model of ERG7 complexed with cation **IV**, which was determined by using the human OSC structure as template, was applied to investigate how changing the structure through mutation affects product profile. Simulated substitution of Trp587 with other amino acid residues showed that this position may stabilize the carbocationic intermediate at the C-6 or C-10 position through CH- π and/or π - π stacking interactions, during A- and B-ring formation. Therefore, substitution of Trp587 with non-aromatic amino acid residues disrupted the above-mentioned interactions and halted the reaction at OS substrate level. In addition, the Trp587 is spatially proximal to the first-tier residues Tyr707, Tyr99 and Phe699 (Fig. 1), which play functional roles in restricting the C-B tricyclic Markovnikov C-14 and/or the rearranged protosteryl C-13/C-17 cation.^{15,17,18} Consistent with the observation is the product profile similarity between W587F and W587Y mutations and those of Y99X and F699X mutations, in which the phenyl/phenolic side chain of Phe or Tyr may partially complement the functional role of the lost indole ring. Furthermore, substitution of the sterically smaller



Scheme 1 The proposed cyclization/rearrangement pathways of oxidosqualene within *S. cerevisiae* ERG7^{Y510X} mutants.

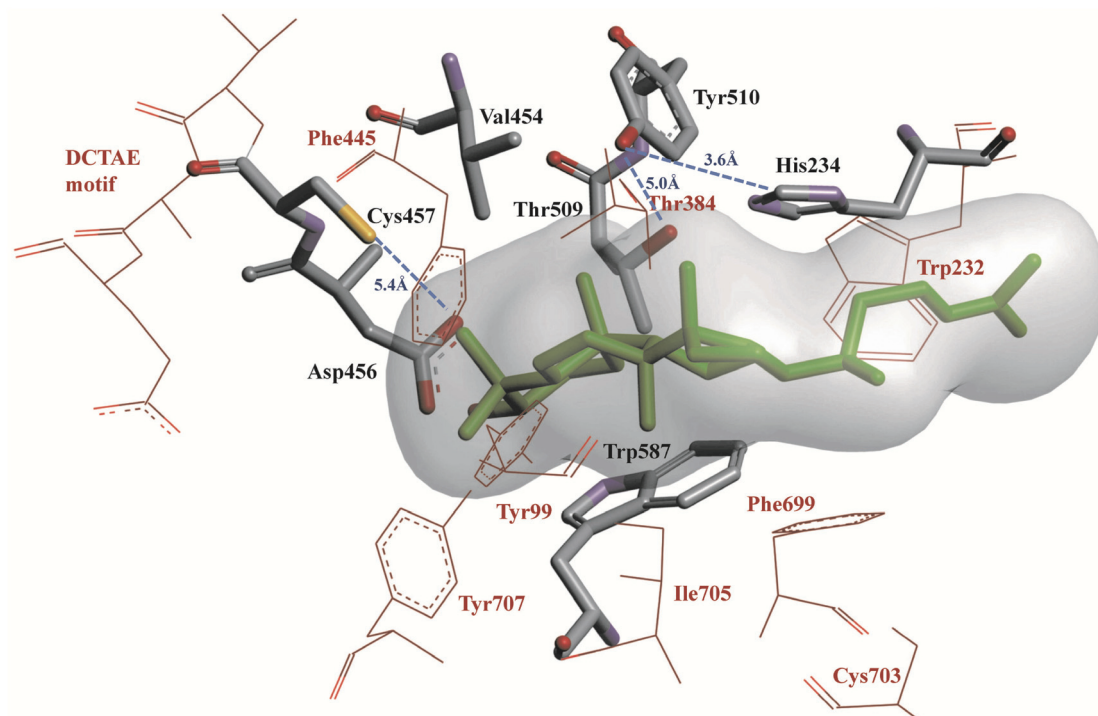


Fig. 1 The homology modeling of ERG7 complexed with C-20 cation intermediate (IV), dotted lines indicate the distances in the putative hydrogen bonding network.

Phe or Tyr side chain might also shift the active site cavity and subsequently affect the orientation or electrostatic interaction of Tyr99 and Phe699, resulting in the formation of compounds 4, 5, and 6. The Cys457 is located next to the Asp456, an essential residue involved in the initiation of ERG7 catalyzed cyclization of OS. Previously, Thoma *et al.* described a H-bonding network among Cys456–Asp455–Cys539 of human OSC with hydrogen bonding distances of 3.9 Å and 3.5 Å between Cys456–Asp456 and Asp456–Cys533, respectively.²⁸ The H-bonding distances between Cys457–Asp456 and Asp456–Cys540 of ERG7 are 5.4 Å and 2.9 Å, respectively. Substitution of Cys457 with aromatic, acidic, and basic amino acid residues disrupted the pre-existing H-bonding to the protonating Asp456, thus abolishing the cyclase activity and any truncated intermediate formation.²⁸ On the other hand, similar to MRN1, in which the highly conserved “DCTAE” motif was replaced with the “DGTAE” motif and a truncated bicyclic product was generated, the C457G mutation produced 3 as the major product. The Gly456 residue in MRN1 has been reported to increase the mobility and basicity of the Asp455 residue in MRN1 and facilitate the deprotonation step.²¹ Perhaps the same substitution in ERG7 may have a similar effect. Similarly, the Thr509 is located next to the Tyr510, a residue putatively involved in forming an H-bonding basic dyad to His234 and affecting the stabilization of various cations. The H-bonding distance in the His234 : Tyr510 basic dyad is 3.6 Å. Substitution of Thr509 with aliphatic, small polar amino acids filled in the space of the Thr residue but slightly affected the hypothetical His234 : Tyr510 dyad, resulting in the formation of the

truncated tricyclic and tetracyclic products 4 or 7. Alternatively, the Thr509 to Gly mutation enlarged the active site cavity and shifted the Tyr510 away from the original position. This, in turn, affected the intrinsic His234 : Tyr510 H-bonding network and the cationic stabilization near the C-10 position of 2, resulting in monocyclic 3 and 8 formation. The abundant generation of the monocyclic products from the substitution of Tyr510 to basic or bulky amino acids might be derived from partial disruption of the transient dipole interaction between C-10 cationic intermediate and the hydroxyl group of the Tyr510, as well as steric or electronic repulsion to the His234 residue. Alternatively, transient disturbance of the His234 : Tyr510 H-bonding dyad by the Tyr510 mutation might cause a shift of Nε2 orientation of the His234 imidazole group away from the C-13 and C-20 protosteryl cations, resulting in the production of tricyclic and altered deprotonation products. Finally, the His234 to Trp and Tyr510 to Trp double mutations might tune the proper orientation of cationic intermediate for the deprotonation reaction to produce achilleol A as its sole product.

Conclusions

In summary, mutational effects of plasticity residues including Cys457, Thr509, Tyr510, His234, and Trp587 that spatially putatively affect OS A-ring cyclization were characterized. Genetic selection and product profile analysis of Trp587 to aromatic amino acid substitutions further supported the

“aromatic hypothesis” that the π -electron-rich pocket is important for the stabilization of electron-deficient cationic intermediates.^{28–33} In addition, substitution of residues next to ERG7-catalyzed OS initiation and/or deprotonation step residues affected the A-ring cyclization when substituted with the small aliphatic residue Gly, possibly through disruption of the pre-existing H-bond to the protonating Asp456 and the intrinsic His234 : Tyr510 H-bonding network, respectively. Furthermore, the successful alteration of ERG7 function to achilleol A synthase activity, through H234W/Y510W double mutation, also supported the concept that a few-ring triterpene synthase could be derived from polycyclic cyclases by reverse evolution. Finally, our results also exemplify the power of computational modeling coupled with protein engineering both to study the enzyme’s structure–function–mechanism relationships and to evolve new enzymatic activity.

Experimental

Generation and analysis of mutant extracts

Site saturated/directed mutagenesis on the respective amino acids, including Trp587, Cys457, Thr509, Tyr510 or His234 in the wild type ERG7 gene was performed using the QuikChange site-directed mutagenesis kit (Stratagene Inc., La Jolla, CA). The oligonucleotide primers used were the following, with substitutions underlined and silent mutation italicized. ERG7^{H234W}-*XhoI*: 5'-d(TGGGTTTGGACTCGAGGTGTTTACATT)-3'; ERG7^{C457X}-*Degenerate1-AIwNI*: 5'-d(GGCTATACAGTGGCTGATNNNACTGCAGAAG)-3'; ERG7^{T509X}-*Degenerate1-BamHI*: 5'-d(TCTTTTGAATATGGATCCTTTGCANNNTATGAAAAAATT)-3'; ERG7^{Y510X}-*Degenerate1-BamHI*: 5'-d(TCTTTTGAATATGGATCCTTTGCAACCNNNGAAAAAATTAAGG)-3'; ERG7^{W587X}-*Degenerate1-BamHI*: 5'-d(GGATCCTGGTATGGAAGCNNNGGTATTTGTTT-TACA)-3'. The recombinant plasmids were subjected to *Dpn* I digestion to remove the parent plasmid, according to the manufacturer’s protocols. The substitutions were determined by DNA sequencing. The mutated ERG7 plasmids were transformed into TKW14C2 strain, an ERG7-deficient yeast strain, by electroporation using a GenPulser with Pulse Controller (BioRad). Aliquots of 120 μ L of each culture were plated onto SD + Ade + Lys + His + Met + Ura + hemin + ergosterol + G418 plates, and re-plated on the same plates, except for the absence of ergosterol, as described previously.^{10,11,13} The pRS314 and pRS314WT were also transformed as negative and positive controls, respectively. The TKW14C2 [pERG7^{mutant}] transformants were grown in SD + Ade + Lys + His + Met + Ura + hemin + ergosterol medium at 30 °C with shaking (150 rpm) for seven to ten days. The non-saponifiable lipids (NSLs) were extracted and fractionated by silica gel column chromatography using a 19:1 hexane–ethyl acetate mixture or by AgNO₃-impregnated silica gel chromatography using 15% diethyl ether in hexane. Each of fractions was checked by thin layer chromatography and applied for the GC and GC-MS analysis. If necessary, the structures of isolated products were characterized

and identified by NMR spectroscopy (¹H, ¹³C, DEPT, COSYDEC, HSQC, HMBC, and NOE).

Molecular modeling studies were performed using the Insight II Homology program with the X-ray structure of lanosterol-complexed human OSC (PDB entry: 1W6K)²⁸ as the template, as previously described.^{10,13} Briefly, the MODELER program was used to extract spatial constraints including stereochemistry, main- and side-chain conformations, distance and dihedral angle. Pairwise sequence alignment between *Sce*ERG7 and human OSC, and between *Sce*ERG7 and bacterial SHC showed 40% and 18% identity, respectively. The resulting model structures were refined by energy minimization until energy convergence by using the SYBYL program (Tripos application software interface). The genetic algorithm (GA) for protein–ligand docking software Gold was chosen to calculate the docking modes of different isolated products in the binding site of the ERG7 homology model.³⁴ A high degree conservation of sequence and good accordance of structure were detected in the putative active site residues among these cyclases, despite low sequence identity in the whole sequence. All software of computational calculation was provided by the Taiwan National Center for High-performance Computing. The reliability of the generated homology models or the specific interaction between ligands and the specific residues within the enzyme active site were examined *via* several geometrical check programs, and their 3D profiles were generated by using the NIH MBI Laboratory Servers at UCLA (<http://nihserver.mbi.ucla.edu/>).^{35–39}

Acknowledgements

We are grateful to Dr John H. Griffin and Prof. Tahsin J. Chow for their helpful advice. We thank the MOE ATU Plan, the National Chiao Tung University as well as the National Science Council of the Republic of China for financial support of this research under Contract No. NSC-99-2113-M-009-008-MY3, and NSC-99-2113-M-009-004-MY2. We thank the National Center for High-Performance Computing for computer time and facilities.

Notes and references

- 1 I. Abe, M. Rohmer and G. D. Prestwich, *Chem. Rev.*, 1993, **93**, 2189–2206.
- 2 K. U. Wendt, G. E. Schulz, E. J. Corey and D. R. Liu, *Angew. Chem., Int. Ed.*, 2000, **39**, 2812–2833.
- 3 R. Xu, G. C. Fazio and S. P. T. Matsuda, *Phytochemistry*, 2004, **65**, 261–291.
- 4 I. Abe, *Nat. Prod. Rep.*, 2007, **24**, 1311–1331.
- 5 E. J. Corey, H. Cheng, C. H. Baker, S. P. T. Matsuda, D. Li and X. Song, *J. Am. Chem. Soc.*, 1997, **119**, 1289–1296.
- 6 B. M. Joubert, L. Hua and S. P. T. Matsuda, *Org. Lett.*, 2000, **2**, 339–341.

- 7 M. M. Meyer, M. J. R. Segura, W. K. Wilson and S. P. T. Matsuda, *Angew. Chem., Int. Ed.*, 2000, **39**, 4090–4092.
- 8 S. Lodeiro, W. K. Wilson, H. Shan and S. P. T. Matsuda, *Org. Lett.*, 2006, **8**, 439–442.
- 9 S. Lodeiro, Q. Xiong, W. K. Wilson, Y. Ivanova, M. L. Smith, G. S. May and S. P. T. Matsuda, *Org. Lett.*, 2009, **11**, 1241–1244.
- 10 T. K. Wu and C. H. Chang, *ChemBioChem*, 2004, **5**, 1712–1715.
- 11 T. K. Wu, Y. T. Liu and C. H. Chang, *ChemBioChem*, 2005, **6**, 1177–1181.
- 12 T. K. Wu, M. T. Yu, Y. T. Liu, C. H. Chang, H. J. Wang and E. W. G. Diau, *Org. Lett.*, 2006, **8**, 1319–1322.
- 13 T. K. Wu, Y. T. Liu, C. H. Chang, M. T. Yu and H. J. Wang, *J. Am. Chem. Soc.*, 2006, **128**, 6414–6419.
- 14 T. K. Wu, Y. T. Liu, F. H. Chiu and C. H. Chang, *Org. Lett.*, 2006, **8**, 4691–4694.
- 15 T. K. Wu, H. Y. Wen, C. H. Chang and Y. T. Liu, *Org. Lett.*, 2008, **10**, 2529–2532.
- 16 T. K. Wu, T. T. Wang, C. H. Chang and Y. T. Liu, *Org. Lett.*, 2008, **10**, 4959–4962.
- 17 T. K. Wu, W. H. Li, C. H. Chang, H. Y. Wen, Y. T. Liu and Y. C. Chang, *Eur. J. Org. Chem.*, 2009, 5731–5737.
- 18 T. K. Wu, C. H. Chang, H. Y. Wen, Y. T. Liu, W. H. Li, T. T. Wang and W. S. Shie, *Org. Lett.*, 2010, **12**, 500–503.
- 19 T. K. Wu, Y. C. Chang, Y. T. Liu, C. H. Chang, H. Y. Wen, W. H. Li and W. S. Shie, *Org. Biomol. Chem.*, 2011, **9**, 1092–1097.
- 20 M. D. Kolesnikova, W. K. Wilson, D. A. Lynch, A. C. Obermeyer and S. P. T. Matsuda, *Org. Lett.*, 2007, **9**, 5223–5226.
- 21 Q. Xiong, W. K. Wilson and S. P. T. Matsuda, *Angew. Chem., Int. Ed.*, 2006, **45**, 1285–1288.
- 22 M. Shibuya, T. Xiang, Y. Katsube, M. Otsuka, H. Zhang and Y. Ebizuka, *J. Am. Chem. Soc.*, 2007, **129**, 1450–1455.
- 23 R. Ito, K. Mori, I. Hashimoto, C. Nakano, T. Sato and T. Hoshino, *Org. Lett.*, 2011, **13**, 2678–2681.
- 24 A. F. Barrero, E. J. R. Alvarez-Manzaneda, M. Mar Herrador, R. Alvarez-Manzaneda, J. Quilez, R. Chahboun, P. Linares and A. Rivas, *Tetrahedron Lett.*, 1999, **40**, 8273–8276.
- 25 A. F. Barrero, E. J. R. Alvarez-Manzaneda and R. Alvarez-Manzaneda, *Tetrahedron Lett.*, 1989, **30**, 3351–3352.
- 26 J. S. Yadav, K. Satyanarayana, P. Sreedhar, P. Srihari, T. B. Shaik and S. V. Kalivendi, *Bioorg. Med. Chem. Lett.*, 2010, **20**, 3814–3817.
- 27 B. A. J. Hess, *J. Am. Chem. Soc.*, 2002, **124**, 10286–10287.
- 28 R. Thoma, T. Schulz-Gasch, B. D'Arcy, J. Benz, J. Aebi, H. Dehmlow, M. Hennig, M. Stihle and A. Ruf, *Nature*, 2004, **432**, 118–122.
- 29 C. J. Buntel and J. H. Griffin, *J. Am. Chem. Soc.*, 1992, **114**, 9711–9713.
- 30 Z. Shi, C. J. Buntel and J. H. Griffin, *Proc. Natl. Acad. Sci. U. S. A.*, 1994, **91**, 7370–7374.
- 31 K. Poralla, A. Hewelt, G. D. Prestwich, I. Abe, I. Reipen and G. Sprenger, *Trends Biochem. Sci.*, 1994, **19**, 157–158.
- 32 D. A. Dougherty, *Science*, 1996, **271**, 163–168.
- 33 T. K. Wu and J. H. Griffin, *Biochemistry*, 2002, **41**, 8238–8244.
- 34 G. Jones, P. Willett and R. C. Glen, *J. Mol. Biol.*, 1995, **245**, 43–53.
- 35 J. Pontius, J. Richelle and S. J. Wodak, *J. Mol. Biol.*, 1996, **264**, 121–136.
- 36 R. Luthy, J. U. Bowie and D. Eisenberg, *Nature*, 1992, **356**, 83–85.
- 37 T. Schulz-Gasch and M. Stahl, *J. Comput. Chem.*, 2003, **24**, 741–753.
- 38 R. A. Laskowski, M. W. MacArthur, D. S. Moss and J. M. Thornton, *J. Appl. Crystallogr.*, 1993, **26**, 283–291.
- 39 A. L. Morris, M. W. MacArthur, E. G. Hutchinson and J. M. Thornton, *Proteins: Struct., Funct., Genet.*, 1992, **12**, 345–364.